Journal of Hazardous Materials 181 (2010) 204–210

Contents lists available at ScienceDirect

Journal of Hazardous Materials

journal homepage: www.elsevier.com/locate/jhazmat

Adsorption of methyl orange and Cr(VI) on mesoporous TiO_2 prepared by hydrothermal method

S. Asuha*, X.G. Zhou, S. Zhao

Chemistry & Environment Science College, Inner Mongolia Normal University, Key Laboratory of Physics and Chemistry of Function Materials, Inner Mongolia, Huhhot 010022, China

ARTICLE INFO

Article history:
Received 19 December 2009
Received in revised form 19 April 2010
Accepted 29 April 2010
Available online 7 May 2010

Keywords:
Adsorption
Water treatment
Mesoporous TiO_2
Methyl orange
Chromium

ABSTRACT

Mesoporous TiO_2 was synthesized by a hydrothermal method using cetyltrimethyl ammonium bromide (CTAB) as a structure-directing agent, and its adsorption abilities for the removal of methyl orange (MO) and Cr(VI) from waste waters were investigated. Transmission electron micrograph (TEM) observations together with nitrogen adsorption–desorption measurements show the formation of mesoporous TiO_2 with an average pore size of 5.2 nm and a surface area of 161.2 m^2/g. The adsorption data for both MO and Cr(VI) fit well with either Langmuir or Freundlich adsorption model. The adsorption for MO is slightly influenced by pH of the solutions, while that for Cr(VI) is strongly dependent on solution pH. By an increase in solution pH from 3 to 12, the adsorbed percentage of MO decreases from ca. 87 to 78%; however, the adsorbed percentage of Cr(VI) decreases from ca. 45 to 0%. The maximum adsorption capacities of the mesoporous TiO_2 for MO and Cr(VI) are determined to be 454.5 and 33.9 mg/g, respectively, which suggests that the mesoporous TiO_2 is an excellent adsorbent for MO and Cr(VI).

1. Introduction

Removal of industrial pollutants from water is becoming more and more important to the world's health, and considerable attention has therefore been paid to water treatments in recent years [1,2]. Industrial waste water generally contains heavy metal ions (e.g., Cr(VI), Hg(II), Pb(II)) and organic pollutants (e.g., azo compounds). Various methods have been developed to remove these pollutants from industrial waste water, e.g., filtration, coagulation–flocculation, reverse osmosis, biological treatment, and distillation, etc. [3–9]. Among these methods, adsorptive filtration is believed to be the most convenient, and it is widely used in water treatment. In this case, filter materials play a key role to efficiently remove industrial pollutants from water. In general, filter materials with high adsorption ability (or high removal capacity) and low cost are employed in practical use. The removal capacity of filter materials depends on their microstructures. Materials with many ion exchange sites and high surface area possess high removal capacities, and they are often used as filter materials. Zeolite is an example of these materials, and it can efficiently remove heavy metal ions from water; but for organic pollutants, the small pore sizes (<1.2 nm) may limit its removal capacity because large organic molecules could not enter the pores. Materials with larger pore sizes than zeolite, therefore, are expected to have high removal capacity for heavy metal ions and organic pollutants. In recent years, Zhong et al. studied application of hierarchically structured iron oxides (i.e., α-Fe_2O_3, γ-Fe_2O_3, and Fe_3O_4) in water treatment, and found their adsorption capacities for As(V) and Cr(VI) were approximately 10 times higher than that of commercial ones [10]. The specific surface areas of these iron oxides were about 20 times higher than that of commercial iron oxides, which may be the most probable reason for high adsorption capacities.

Mesoporous materials, whose pore sizes range from 2 to 50 nm, are of interest because of their potential use in various fields such as heterogeneous catalysis, energy, biotechnology, and nanodevices [11–13]. Owing to their large pore sizes and high surface areas, mesoporous materials are also promising adsorbents for various pollutants in water. From a viewpoint of practical use, the adsorbents themselves should readily be prepared and they should not be toxic. TiO_2, a nontoxic material, satisfies these requirements. Another advantage of TiO_2 is that high concentration of hydroxyl groups (OH) are present on the surface, and the pollutants in water can be adsorbed on the TiO_2 surface via interacting with surface OH. In fact, TiO_2 nanomaterial recently has been developed for effective adsorbent of arsenic, showing higher removal capacities than bulk material [14]. Mesoporous TiO_2 is expected to possess higher removal capacities than non-porous TiO_2 because of its high surface area and highly porous structure. In fact, mesoporous TiO_2 has been found to be an effective adsorbent for organic compounds with carboxy groups [15]. Since the first report of the synthesis

* Corresponding author. Tel.: +86 471 43921214; fax: +86 471 4392124.
E-mail addresses: asuha42@yahoo.com.cn, asuha@imnu.edu.cn (S. Asuha).

0304-3894/$ – see front matter © 2010 Elsevier B.V. All rights reserved.
doi:10.1016/j.jhazmat.2010.04.117

of mesoporous TiO_2 in 1995, it has attracted much attention for many different applications, including photocatalysts, solar cells, biomaterials, and environmental catalysts [16,17]. It is also known that most of the previous studies are focused on photocatalytic properties of mesoporous TiO_2 [18–20]. On the other hand, up to now, extensive studies on the adsorption properties of pure mesoporous TiO_2 have not been performed in view of application to water treatment. Xie et al. studied the adsorption and photocatalytic degradation of MO on mesoporous F–N-codoped TiO_2 powder and found that the adsorption capacity of the powder was much higher than that of Deggusa P25 [21]. But in that case, the detailed adsorption mechanism was not given. We think that the adsorption mechanism may differ from that for pure mesoporous TiO_2 powder because of the presence of F and N.

In the present study, mesoporous TiO_2 was synthesized by a hydrothermal method, and its adsorption abilities for Cr(VI) and methyl orange (MO) were investigated in view of application to water treatment. Here Cr(VI) and MO were selected as typical heavy metal ions and azo compounds (i.e., organic pollutants in waste water), respectively. In synthesis, titanium sulfate ($Ti(SO_4)_2$) was used as the precursor of TiO_2, and cationic surfactant cetyltrimethyl ammonium bromide (CTAB) as a structure-directing agent. The obtained TiO_2 exhibited wormhole-like disordered structure with a narrow pore size distribution and a very high surface area. For comparison, the adsorption abilities of commercial TiO_2, a non-mesoporous material, were also investigated at the same conditions as those used for mesoporous TiO_2.

2. Experimental

2.1. Materials

$Ti(SO_4)_2$ (98%, National Chemicals), absolute ethanol (99%, Beijing Chemical Reagents Company), cetyltrimethyl ammonium bromide (CTAB, 99%, Beijing Chemical Reagents Company), methyl orange (MO, 99%, China Medicine Company), potassium dichromate (99.8% $K_2Cr_2O_7$, Shanghai Fujiang Chemicals Company) were used as received. Commercial TiO_2 with an average particle size of 12 nm and surface area of 45 m^2/g was used for reference.

2.2. Synthesis of TiO_2 materials

Mesoporous TiO_2 was synthesized by a hydrothermal method as follows: 0.55 g of CTAB and 4.32 g of titanium sulfate were dissolved in 30 mL of deionized water under intense stirring; then, the obtained solution was transferred into a 50-mL stainless autoclave with a Teflon liner, followed by heating in an oven at 110 °C for 24 h. The precipitate was separated from the solution by filtering and rinsed with deionized water and ethanol several times. Finally, the precipitate was dried in an oven at 80 °C, resulting in the formation of a white powder.

2.3. Characterization

X-ray diffraction patterns (XRD) were recorded using a Philips PW 1830 diffractometer with a Cu Kα radiation source. Transmission electron micrograph (TEM) observations were carried out using a JEOL JEM-2010 transmission electron microscope. Nitrogen adsorption–desorption isotherms were measured using a Micrometrics ASAP2020 Analyzer. Brunauner–Emmett–Teller (BET) surface area was calculated from the adsorption branches, and the pore size distribution from the desorption branches using the Barrett–Joyner–Halenda (BJH) method.

2.4. MO and Cr(VI) adsorption

Firstly, aqueous solutions containing different concentrations of MO (5–1000 mg/L) and Cr(VI) (5–100 mg/L) were prepared. In this case, $K_2Cr_2O_7$ was used as the source of Cr(VI). The pH of solution was adjusted by addition of NaOH, HCl or H_2SO_4 solutions, and all adsorption experiments were carried out at room temperature. For the adsorption rate tests, 20 and 50 mg mesoporous TiO_2 adsorbents were added to 20 mL of MO (100 mg/L) and Cr(VI) (50 mg/L) solutions, respectively, under stirring, and stirring was continued for a certain time at room temperature. In this case, the pH of MO and Cr(VI) solutions were adjusted to 5 and 6, respectively. After adsorption process, solid and liquid were separated by centrifugation of the resulting suspension to measure the concentrations of MO and Cr(VI) in the solution. In pH effect studies, the same weight of adsorbent, volume and initial concentration of MO and Cr(VI) solutions as used in the adsorption rate tests were used. In this case, the contact time of adsorbent with solution was set at 20 min. For adsorption isotherm studies, the 20 mL of MO and Cr(VI) with different concentrations were mixed with 20 and 50 mg mesoporous TiO_2 adsorbents for 20 min, respectively. The pH of MO and Cr(VI) solutions were maintained at 5 and 6, respectively. The measurements of MO and Cr(VI) concentrations were carried out using a Shimadzu UV–Vis 2550 spectrophotometer. The MO concentration was determined by measuring the solution absorbance at 466 nm. Diphenylcarbazide spectrophotometric method was used for determination of Cr(VI) concentration.

2.5. Regeneration

The regeneration of mesoporous TiO_2 adsorbent containing MO or Cr(VI) was examined by a chemical desorption method. After adsorption process, the 20 mg collected adsorbent containing MO or Cr(VI) was added to 60 mL 1.0 M NaOH solution under stirring, and stirring was continued for 2 h at room temperature. After removing from NaOH solution, the adsorbent was washed with 0.05 M acetic acid solution and deionized water; then, it was dried at 80 °C. The regenerated adsorbent was further used for adsorption–desorption test.

For all adsorption tests, 100 mg/L MO (pH 5) and 50 mg/L Cr(VI) (pH 6) solutions were used; and the contact time of adsorbent with solution was set at 20 min.

3. Results and discussion

3.1. Synthesis of mesoporous TiO_2

Fig. 1 shows the XRD pattern of mesoporous TiO_2. The diffraction pattern matches well with the JCPDS file (e.g., No. 71-1167) of anatase, and the diffraction peaks of which are quite sharp, indicating the formation of well crystallized anatase phase. The average crystalline size calculated from the half-width of the diffraction lines using the Scherrer's equation was about 11.7 nm. Fig. 2 shows the TEM micrograph of mesoporous TiO_2. It is clearly seen that the TiO_2 particles do not have a defined shape. Disordered wormhole-like arrangement of pores is clearly observed on each particle, indicating the formation of mesoporous structure.

The nitrogen adsorption–desorption isotherms of the TiO_2 powder are shown in Fig. 3. The inset shows the BJH pore size distribution plot. The shapes of these isotherms approximately agree with type IV isotherm. In addition, a hysteresis loop due to capillary condensation was also observed for adsorption and desorption branches. According to previous studies, mesoporous materials usually exhibit type IV-like isotherms with a hysteresis loop [17,22,23]. Therefore, the result of nitrogen adsorption–desorption

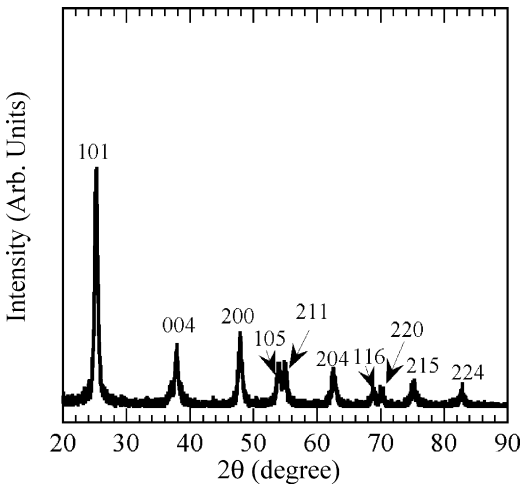

Fig. 1. XRD pattern for mesoporous TiO_2.

further confirms that our sample has mesoporous structure. From the adsorption isotherm, the BET surface area of the sample was estimated to be 161.2 m^2/g. As shown in BJH curve, the pore sizes were in the range between 3 and 10 nm, with an average pore size of 5.2 nm and a pore volume of 0.33 cm^3/g.

3.2. Absorption behavior of MO and Cr(VI) on mesoporous TiO_2

3.2.1. Adsorption kinetics

Fig. 4 shows the adsorption rate curves of MO and Cr(VI) on mesoporous TiO_2. For comparison, the curves for commercial TiO_2 are also shown in the figure. For both MO and Cr(VI), the adsorption reached equilibrium within 20 min; the maximum adsorbed percentages for MO and Cr(VI) on mesoporous TiO_2 were 89 and 53%, respectively. The result indicates that more than 90% of MO in the solution could be removed in a short time when the mesoporous TiO_2 is used as an adsorbent. In addition, the adsorbed percentages of MO and Cr(VI) on the mesoporous TiO_2 were 11 and 3 times larger than those on commercial TiO_2, showing the mesoporous TiO_2 had much higher adsorption abilities than commercial TiO_2. The specific surface area of our sample is about 4 times larger than that

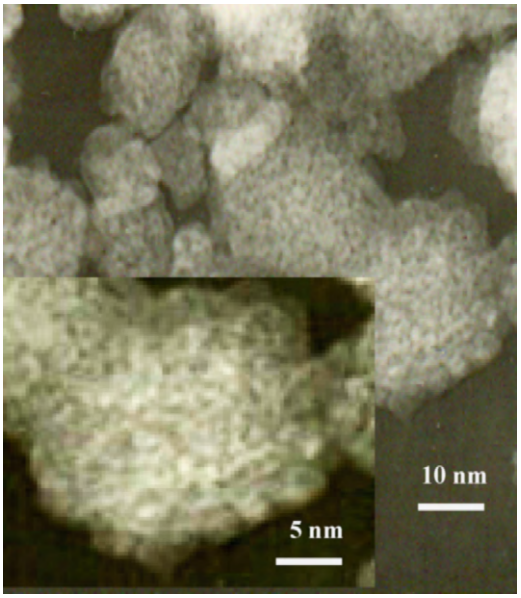

Fig. 2. TEM micrograph of mesoporous TiO_2.

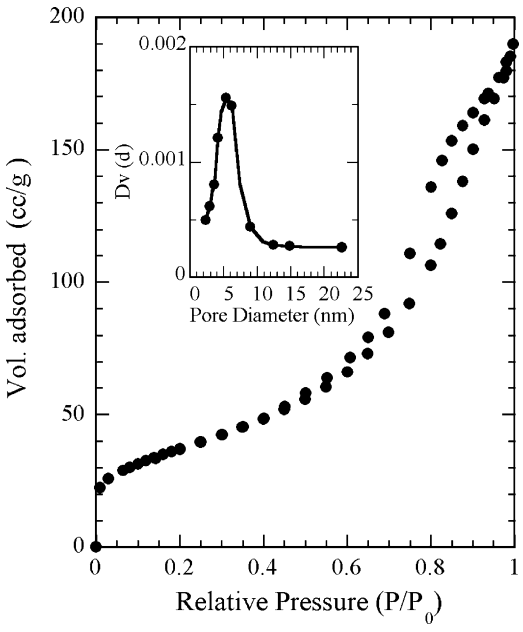

Fig. 3. Nitrogen adsorption–desorption isotherms for mesoporous TiO_2. BJH pore size distribution is shown in the inset.

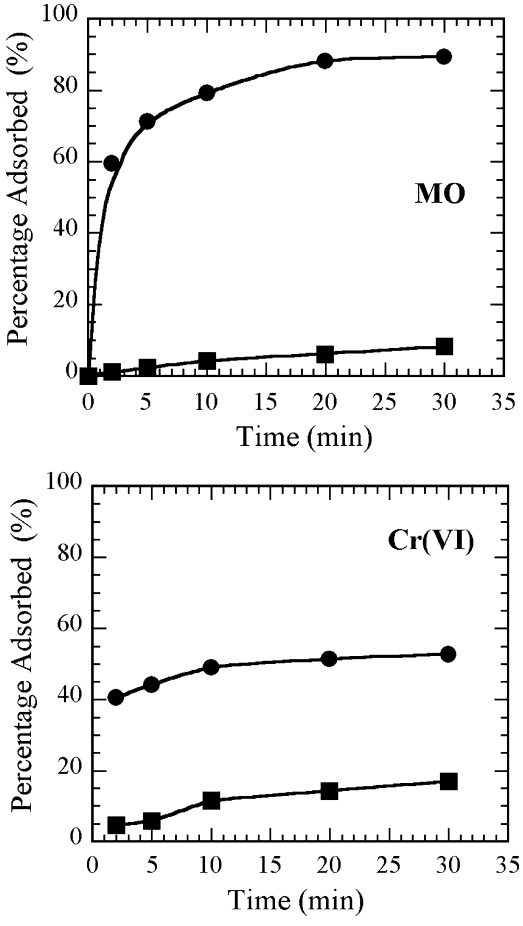

Fig. 4. Adsorption rate curves for MO and Cr(VI). Circles are for mesoporous TiO_2; squares are for commercial TiO_2.

Fig. 5. Photographs of the MO solutions: (a) without addition of mesoporous TiO_2; (b) with addition of mesoporous TiO_2.

of commercial TiO_2; this may be the probable reason for the high adsorption abilities. Fig. 5 shows the photographs of the MO solutions. Photographs (a) and (b) were for the MO solutions (100 mg/L) without and with the addition of mesoporous TiO_2, respectively. After adsorption process, the MO solution with yellow color became nearly colorless, indicating that the most of MO in the solution was adsorbed on mesoporous TiO_2.

3.2.2. Effect of solution pH on MO and Cr(VI) adsorption

The solution pH is one of the key factors which may influence adsorption performance and adsorption mechanism. In order to investigate the effect of solution pH on the adsorption capacity of the mesoporous TiO_2, a set of adsorption experiments were performed at various solution pH conditions. Fig. 6 shows the adsorbed percentages of MO and Cr(VI) on the mesoporous TiO_2 vs. pH. For both MO and Cr(VI), the adsorbed percentages at low pH were larger

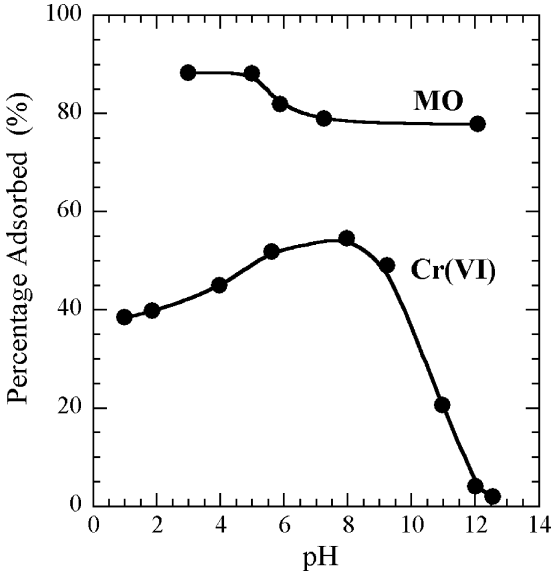

Fig. 6. The effect of solution pH on adsorbed percentages of MO and Cr(VI).

than those at high pH. In addition, the effect of solution pH for MO and Cr(VI) adsorption were different. When the solution pH was varied from 3 to 12, the adsorbed percentage of MO decreased from ca. 87 to 78%; however, the adsorbed percentage of Cr(VI) decreased from ca. 45 to 0%. This discrepancy suggests the presence of different adsorption mechanisms for MO and Cr(VI) adsorption.

MO is a polar molecule, and therefore it could be adsorbed on the surface of TiO_2 via van der Waals force. In addition, O, N, and S atoms in MO could form hydrogen bonds, due to their high electronegativities, with the surface hydroxyl groups of TiO_2. According to previous study, the concentration of the surface hydroxyl groups of TiO_2 strongly depends on solution pH [24]. When the solution pH is low, they are mainly present in the forms of Ti-OH and/or Ti-OH_2^+, resulting in the formation of hydrogen bonds with MO molecules. Therefore, we think that both van der Waals force and hydrogen bond formation are contributive to MO adsorption. When the solution pH is high, on the other hand, the surface hydroxyl groups of TiO_2 will be dissociated to form TiO^-; hence, no hydrogen bonds thought to be formed between MO and TiO_2 surface. In this case, however, only van der Waals force contributes to MO adsorption. The above argument is in good agreement with the result that the adsorbed percentages for MO in the low pH region are larger than in the high pH region.

In the case of Cr(VI) adsorption, the electrostatic attraction or repulsion between the surface hydroxyl groups of TiO_2 and CrO_4^{2-} (or $Cr_2O_7^{2-}$) dominate the adsorption. When the solution pH is low, negatively charged CrO_4^{2-} or $Cr_2O_7^{2-}$ can associate with TiO_2 surfaces via electrostatic attraction with positively charged Ti-OH_2^+, leading to adsorption. In the high pH region, there will be an electrostatic repulsion between negatively charged CrO_4^{2-} and TiO^-, resulting in the decrease in the adsorption. It should be noted that the maximum adsorbed percentage is observed in Fig. 6. The decrease in the adsorbed percentage with a reduction of solution pH in the low pH region can be explained from the following relation between CrO_4^{2-} and $Cr_2O_7^{2-}$ in aqueous solutions:

$$2CrO_4^{2-} + 2H^+ \rightleftharpoons Cr_2O_7^{2-} + H_2O \quad (1)$$

When the concentration of H^+ ions is high (i.e., low pH), CrO_4^{2-} ions are transferred to $Cr_2O_7^{2-}$ with a high probability, i.e., lowering solution pH enhances the formation of $Cr_2O_7^{2-}$. It is obvious that the dimension of a $Cr_2O_7^{2-}$ ion is about twice as large as a CrO_4^{2-} ion. The large size of a $Cr_2O_7^{2-}$ ion makes it difficult to enter the pores on mesoporous TiO_2, resulting in the lower adsorption capacity.

3.2.3. Adsorption isotherms

The adsorption isotherms of MO and Cr(VI) for the mesoporous TiO_2 are shown in Fig. 7. In the low concentration region, the adsorption capacities for both MO and Cr(VI) linearly increased with the increase of their initial concentrations; and then the increases of the adsorption capacities were retarded in the high concentration region. Langmuir and Freundlich adsorption models, two well-known models, were employed to the analysis of our experimental data. For this, the following Eqs. (2) and (3) were used for Langmuir and Freundlich adsorption model studies, respectively [25,26].

$$\frac{C_e}{q_e} = \frac{1}{k_L q_m} + \frac{C_e}{q_m} \quad (2)$$

$$\ln q_e = \ln k_F + \frac{1}{n \ln C_e} \quad (3)$$

where C_e is the equilibrium concentration of adsorbate, q_e is the equilibrium adsorption capacity, k_L is the Langmuir adsorption equilibrium constant, q_m is the maximum adsorption capacity, k_F is the Freundlich adsorption equilibrium constant, and n is

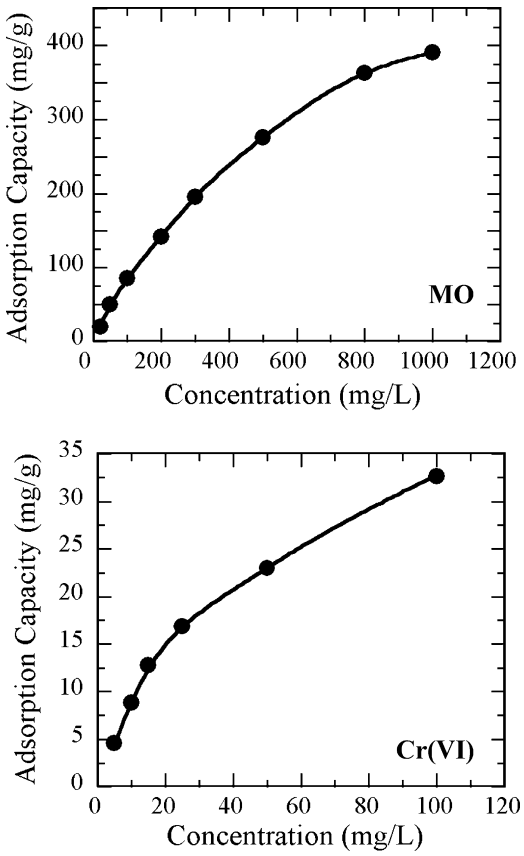

Fig. 7. Adsorption isotherms for MO and Cr(VI).

the constant of Freundlich adsorption. The Langmuir and Freundlich adsorption isotherms that are obtained using above two equations are given in Fig. 8. As seen in the figure, good linear relations are obtained for MO and Cr(VI), indicating that our experimental data fit well with either the Langmuir or the Freundlich adsorption model. In the case of MO adsorption, the correlation coefficients (R^2) for Langmuir and Freundlich adsorption isotherms were 0.9839 and 0.9955, respectively. This indicates that the experimental data has a better fit with the Freundlich adsorption model. As discussed above, MO is adsorbed on the TiO_2 surface by means of van der Waals force and hydrogen bond formation at the low pH condition. The presence of these two kinds of adsorption sites may be the most probable reason for better fit with Freundlich adsorption model, since this model is the summation of adsorption on all surface sites with different bonds. In the case of Cr(VI) adsorption, however, the R^2 for Langmuir and Freundlich adsorption isotherms were 0.9952 and 0.9512, respectively, indicating that obtained data fit with Langmuir adsorption model better. This implies that the adsorbed layer is monolayer coverage. As mentioned above, Cr(VI) is adsorbed on the TiO_2 surface via the electrostatic attraction between the surface hydroxyl groups of TiO_2 and CrO_4^{2-}. Thus, the homogeneous nature of surface hydroxyl groups led to Langmuir type adsorption. From Langmuir adsorption isotherms, the maximum adsorption capacities of the mesoporous TiO_2 for MO and Cr(VI) were estimated to be 454.5 mg/g (or 1.39 mmol/g) and 33.9 mg/g (or 0.25 mmol/g), respectively. These values are almost one order larger than those obtained for hierarchically structured iron oxides [10]. The maximum capacity for Cr(VI) is only slightly smaller than the value (0.35 mmol/g) obtained for chemically modified mesoporous silica (SBA-15) [27], although the BET surface area of our sample is approximately 4 times lower than the chemically modified mesoporous silica.

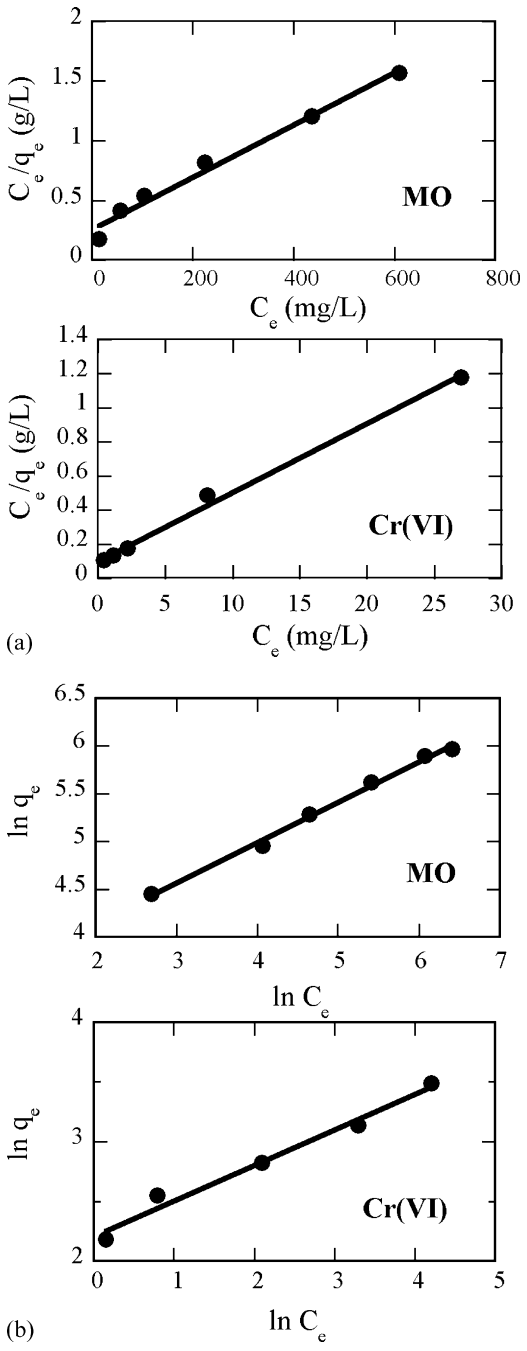

Fig. 8. Langmuir adsorption isotherms (a) and Freundlich adsorption isotherms (b).

3.2.4. *Regeneration of the mesoporous TiO_2 adsorbent*

In order to investigate the reusability of the mesoporous TiO_2, cyclic adsorption–regeneration tests were carried out for MO and Cr(VI). Fig. 9 shows the removal abilities of mesoporous TiO_2 for MO and Cr(VI) during several adsorption–regeneration cycles. For both MO and Cr(VI), the removal abilities markedly decreased in the initial two cycles; and then the decreases were retarded in the subsequent recycling. After five cycles, the adsorption capacities for MO and Cr(VI) were still maintained at 17 and 14 mg/g, respectively; these values were much larger than those of commercial TiO_2. In addition, the magnitudes of the decrease in the removal ability for MO and Cr(VI) after five cycles were much different, i.e., the adsorbed percentage of MO decreased markedly from 89 to 16%, while that of Cr(VI) decreased from 53 to 28%. This result can be explained from the adsorption mechanism of MO or Cr(VI) on

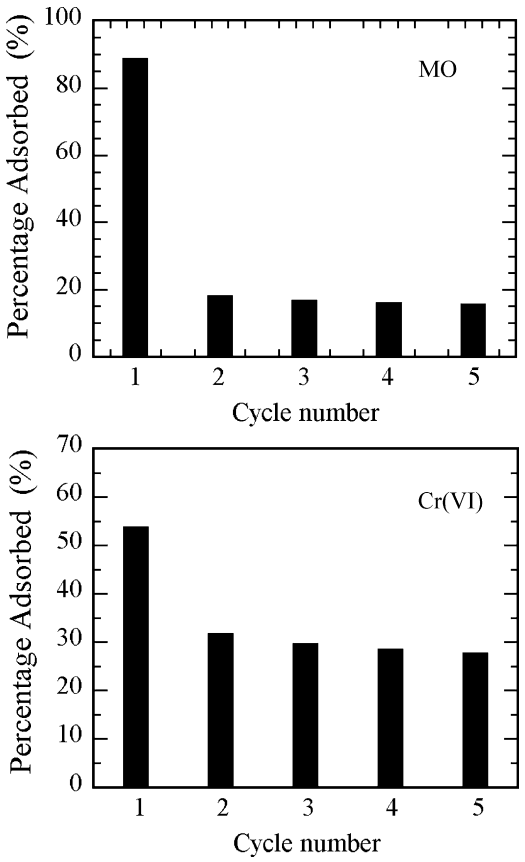

Fig. 9. Reusability of mesoporous TiO_2 adsorbent.

the mesoporous TiO_2. As shown in Fig. 6, the adsorption of MO was only slightly influenced by solution pH, and adsorbed percentage of MO was as high as 78% even at pH 12. This, in turn, implies that the desorption of MO is difficult to occur in a base (i.e., NaOH), which is responsible for the large decrease of adsorption capacity of the mesoporous TiO_2 for MO. In the case of Cr(VI) adsorption, however, the adsorbed percentage was ca. 0% at high pH, indicating that adsorbed Cr(VI) can be desorbed using NaOH solution. Consequently, the complete desorption of Cr(VI) in NaOH solution leads to a less decrease in the removal ability. The regeneration capacity of the material for Cr(VI) is sufficient, but that for MO needs improvement.

4. Conclusions

Mesoporous TiO_2 is studied in view of its application to water treatment and the following results and conclusions are obtained:

(1) In comparison with commercial TiO_2, the mesoporous TiO_2 shows much higher adsorption abilities for MO and Cr(VI), and it is attributed to its high surface area.
(2) For both MO and Cr(VI), the adsorbed percentages at low pH are larger than those at high pH.
(3) The adsorption for MO is slightly influenced by solution pH, while that for Cr(VI) is strongly dependent on solution pH.
(4) For MO adsorption, both van der Waals force and hydrogen bond formation are contributive to adsorption; while for Cr(VI) adsorption, the electrostatic attraction or repulsion between the surface hydroxyl groups of TiO_2 and CrO_4^{2-} dominate the adsorption.
(5) The adsorption data for both MO and Cr(VI) fit well with either the Langmuir or the Freundlich adsorption isotherms. For MO adsorption, fit with Freundlich adsorption model better; however, the adsorption of Cr(VI) has a better fit with Langmuir adsorption model.
(6) The mesoporous TiO_2 adsorbent containing Cr(VI) can be effectively regenerated by a chemical desorption method using NaOH solution. The regeneration of mesoporous TiO_2 adsorbent containing MO needs further improvement.

Acknowledgments

This work was financially supported by National Natural Science Foundation of China (Grant No. 20861006) and Talent Foundation of Inner Mongolia.

References

[1] J.S. Hu, L.S. Zhong, W.G. Song, L.J. Wan, Synthesis of hierarchically structured metal oxides and their application in heavy metal ion removal, Adv. Mater. 20 (2008) 2977–2982.
[2] A.R. Samarkandy, Kh.M. Mostafa, Synthesis and development of novel aminated chelating resin and its application in industrial waste water treatment, Aust. J. Basic Appl. Sci. 3 (2009) 1772–1779.
[3] G. Crini, Recent developments in polysaccharide-based materials used as adsorbents in wastewater treatment, Prog. Polym. Sci. 30 (2005) 38–70.
[4] S.M. Xu, S. Feng, G. Peng, J.D. Wang, A. Yushan, Removal of Pb (II) by crosslinked amphoteric starch containing the carboxymethyl group, Carbohydr. Polym. 60 (2005) 301–305.
[5] V.K. Guptaa, C.K. Jainb, I. Alib, M. Sharmaa, V.K. Saini, Removal of cadmium and nickel from wastewater using bagasse fly ash—a sugar industry waste, Water Res. 37 (2003) 4038–4044.
[6] C.I. Pearcea, J.R. Lloydb, J.T. Guthrie, The removal of colour from textile wastewater using whole bacterial cells: a review, Dyes Pigments 58 (2003) 179–196.
[7] B.V.D. Bruggen, C. Vandecasteele, Removal of pollutants from surface water and groundwater by nanofiltration: overview of possible applications in the drinking water industry, Environ. Pollut. 122 (2003) 435–445.
[8] R.Y. Ning, Arsenic removal by reverse osmosis, Desalination 143 (2002) 237–241.
[9] Y. Fu, T. Viaraghavan, Fungal decolorization of dye wastewaters: a review, Bioresour. Technol. 79 (2001) 251–262.
[10] L.S. Zhong, J.S. Hu, H.P. Liang, A.M. Cao, W.G. Song, L.J. Wan, Self-assembled 3D flowerlike iron oxide nanostructures and their application in water treatment, Adv. Mater. 18 (2006) 2426–2431.
[11] M. Hartmann, Ordered mesoporous materials for bioadsorption and biocatalysis, Chem. Mater. 17 (2005) 4577–4593.
[12] M.A. Carreon, V.V. Guliants, Ordered meso- and macroporous binary and mixed metal oxides, Eur. J. Inorg. Chem. 1 (2005) 27–43.
[13] S.W. Boettcher, J. Fan, C.K. Tsung, Q.H. Shi, G.D. Stucky, Harnessing the sol–gel process for the assembly of non-silicate mesostructured oxide materials, Acc. Chem. Res. 40 (2007) 784–792.
[14] M. Pena, X. Meng, G.P. Korfiatis, C. Jing, Adsorption mechanism of arsenic on nanocrystalline titanium dioxide, Environ. Sci. Technol. 40 (2006) 1257–1262.
[15] C. Pérez León, L. Kador, B. Peng, M. Thelakkat, Characterization of the adsorption of Ru-bpy dyes on mesoporous TiO_2 films with UV–Vis, Raman, and FTIR spectroscopies, J. Phys. Chem. B 110 (2006) 8723–8730.
[16] D.M. Antonelli, Y.J. Ying, Synthesis of hexagonally packed mesoporous TiO_2 by a modified sol–gel method, Angew. Chem. Int. Ed. Engl. 34 (1995) 2014–2017.
[17] D. Huang, Y.J. Wang, Y.C. Cui, G.S. Luo, Direct synthesis of mesoporous TiO_2 and its catalytic performance in DBT oxidative desulfurization, Microporous Mesoporous Mater. 116 (2008) 378–385.
[18] N. Lakshminarasimhan, E. Bae, W. Choi, Enhanced photocatalytic production of H_2 on mesoporous TiO_2 prepared by template-free method: role of interparticle charge transfer, J. Phys. Chem. C 111 (2007) 15244–15250.
[19] H. Li, Z. Bian, J. Zhu, Y. Huo, H. Li, Y. Lu, Mesoporous Au/TiO_2 nanocomposites with enhanced photocatalytic activity, J. Am. Chem. Soc. 129 (2007) 4538–4539.
[20] D.S. Kim, S.Y. Kwak, The hydrothermal synthesis of mesoporous TiO_2 with high crystallinity, thermal stability, large surface area, and enhanced photocatalytic activity, Appl. Catal. A 323 (2007) 110–118.
[21] Y. Xie, X. Zhao, Y. Li, Q. Zhao, X. Zhou, Q. Yuan, CTAB-assisted synthesis of mesoporous F–N-codoped TiO_2 powders with high visible-light-driven catalytic activity and adsorption capacity, J. Solid State Chem. 181 (2008) 1936–1942.
[22] A. Bhaumik, S. Inagaki, Mesoporous titanium phosphate molecular sieves with ion-exchange capacity, J. Am. Chem. Soc. 123 (2001) 691–696.
[23] M.P. Kapoor, A. Bhaumik, S. Inagaki, K. Kuraoka, T. Yazawa, Titanium containing inorganic–organic hybrid mesoporous materials with exceptional activity in epoxidation of alkenes using hydrogen peroxide, J. Mater. Chem. 12 (2002) 3078–3083.

[24] S. Chibowski, M. Paszkiewicz, Studies of some properties and the structure of polyethylene glycol (PEG) macromolecules adsorbed on a TiO_2 surface, Adsorp. Sci. Technol. 19 (2001) 397–407.
[25] I. Langmuir, The adsorption of gases on plane surfaces of glass, mica and platinum, J. Am. Chem. Soc. 40 (1918) 1361–1403.
[26] H.M.F. Freundlich, Over the adsorption in solution, Z. Phys. Chem. 57 (1906) 385–471.
[27] D. Pérez-Quintanilla, I. del Hierro, M. Fajardo, I. Sierra, Cr(VI) adsorption on functionalized amorphous and mesoporous silica from aqueous and non-aqueous media, Mater. Res. Bull. 42 (2007) 1518–1530.